Desalination and Water Treatment
www.deswater.com
doi: 10.5004/dwt.2018.22830

127 (2018) 197–212
September

Fouling mechanisms in nanofiltration membranes for the treatment of high DOC and varying hardness water

Nisha Jha*, Zsolt László Kiss, Beata Gorczyca

Department of Civil Engineering, Faculty of Engineering, University of Manitoba, 15 Gillson Street, Winnipeg, Manitoba, R3T 5V6, Canada, Tel. +1-4164320032; emails: nisha85np@gmail.com, jhan@myumanitoba.ca (N. Jha), zsoltkiss027@gmail.com (Z.L. Kiss), beata.gorczyca@umanitoba.ca (B. Gorczyca)

Received 6 February 2018; Accepted 22 July 2018

ABSTRACT

This study investigates the behavior of flux decline and change in fouling mechanisms in nanofiltration membranes, for the treatment of high dissolved organic carbon (DOC) water in the presence of divalent cations (Ca^{2+}) at different concentrations. A model synthetic water composed of sodium alginate concentration of 17 mg/L as DOC and calcium chloride of three concentrations: low 50, medium 200, and high 350 mg/L as $CaCO_3$, was used for the fouling study. The synthetic water quality was based on the DOC and hardness concentrations reported in three potable water sources in the Province of Manitoba and Ontario, Canada. A thin-film composite (TFC) NF90 membrane (DOW Filmtec., USA) was used for the fouling studies. Resistance-in-series model and other fouling models were used to describe the permeate flux decline and changing fouling mechanisms in NF90 membranes. The fouling study demonstrated that low calcium concentration formed an irreversible fouling layer with a relatively low surface roughness of 15.38 nm. This was attributed to high adhesive forces between the foulant (primarily alginate molecules) and the rough membrane surface. At high calcium concentration, a dense, compact and reversible fouling layer was formed, due to increased cohesive forces between calcium and alginate molecules, resulting in maximum Ca-Alginate complexation and aggregation. The aggregates further linked together to form a cross-linked foulant structure with a surface, roughness of 38.17 nm. However, for medium calcium concentration a complex (non-uniform porosity) matrix of foulants was formed with a very high surface roughness of 67.97 nm, due to the insufficient calcium available to fulfill the binding sites on alginate molecules. The fouling layer so formed resulted in offering highest flux decline and total hydraulic resistance. Results of fouling experiments identified that the reversibility of alginate fouling increased with increasing calcium concentration. However, the flux decline and the total hydraulic resistance were dependent on both alginate and calcium concentrations for maximum complexation and aggregation. In addition to the aforementioned effects of Ca^{2+}, results also show that the dominance of gel layer formation fouling mechanism increases with increase in calcium concentrations.

Keywords: Nanofiltration; Surface water; DOC; Hardness; Ca-alginate complexation; Fouling mechanisms; Gel layer

1. Introduction

Surface water sources in the Provinces of Manitoba and Ontario (Canada) have been reported to contain high concentrations of dissolved organic carbon (DOC) and wide range of hardness levels. Therefore, the removal of DOC and hardness has been one of the major objectives for many of the drinking water treatment plants (WTP) in the area. NF membranes have been found to be highly efficient in the treatment of these surface waters, due to its high retention potential for organics and inorganics (especially divalent cations), and high flux production [1]. However, NF membranes are highly susceptible to fouling, thus, limiting the successful application of the membrane technology. Fouling of membranes

* Corresponding author.

can cause reduction of permeate flux or increase in operating pressures, that requires use of effective pretreatment methods, frequent chemical cleaning, reduced membrane life leading to membrane replacement, ultimately affecting the energy requirements, and the plant economy [2–6].

The fouling process and mechanisms are highly influenced by membrane characteristics, feed water composition, natural organic matter (NOM) properties, and hydrodynamic and operating conditions [7–9]. Most of the NF membranes are typically designed to be negatively charged at neutral pH [10] and both, charge effects and size exclusion mechanisms influence the rejection behavior in NF membranes [11,12]. Flux decline in NF membranes can occur due to the accumulation of high concentration of pollutants near the membrane surface due to diffusion (concentration polarization), formation of a gel layer on the membrane surface or pore restriction and blocking by molecules in water that can penetrate into the membrane pores. The mechanisms of fouling in NF membranes have been characterized most commonly using resistance-in-series model [13,14]. The fouling in NF membranes can be both reversible and irreversible (after chemical cleaning) [15], depending on the fouling mechanisms and interactions between the foulants and membrane. The occurrence of these fouling mechanisms is not completely independent of each other, and therefore the effect of each mechanism needs to be studied individually to observe its contribution to the decreased membrane performance [16].

1.1. Feed water composition and membrane fouling

Surface waters comprise of a complex mixture of various compounds but most important for membrane filtration are NOM (typically reported as DOC) and divalent cations (primarily Ca^{2+} and Mg^{2+}) contributing hardness [17]. The composition of NOM in surface water depends on the seasonal changes and source of origin. Dissolved NOM is considered to be the major cause of NF fouling during filtration of surface waters [1,7,10,18]. Dissolved NOM is generally comprised of humic substances, polysaccharides, amino acids, fatty acids, proteins, etc., NOM can be fractionated into three major components, hydrophobic, hydrophilic, and transphilic (acid, base, or neutral), where hydrophilic neutral compounds (such as polysaccharides and proteins) are reported to have the highest fouling potential [19–22].

Along with NOM in surface water, another predominant compound present is the variety of inorganic salts and minerals. Divalent cations such as Ca^{2+} and Mg^{2+} are mainly responsible for imparting hardness to the water. These alkaline earth metal cations when combined with polyanions such as carbonate (CO_3^{2-}), sulfate (SO_4^{2-}), and phosphate (PO_4^{3-}) ions, can lead to more fouling problems on NF membranes [23]. The presence of high hardness concentration in surface water can result in scaling [16]. Membrane scaling is a very common phenomenon occurring at the membrane surface, mostly in NF and RO systems. Some of the most commonly found inorganic salts that are responsible for scale formation on the membrane surface are $CaSO_4$, $CaCO_3$, SiO_2, and $BaSO_4$ [24]. The precipitation of these inorganic salts at the membrane surface and pores result in significant flux decline (decreased permeate recovery). Jarusuthirak et al. [23] reported a decline in flux of 40% and 43% in NF membranes for feed waters containing CO_3^{2-} and SO_4^{2-} species, respectively. Silica, on the other hand, is less common but equally problematic for treatment depending on the pH and temperature of the feed water [24].

Scaling in membranes can be prevented by use of low operating pressures. The formation of concentration polarization layer is minimum at low operating pressures, which also decreases the surface crystallization, thus preventing scaling [25]. Scaling issues can further be alleviated or controlled by pH adjustment, acid and antiscalant addition [26]. Several types of antiscalants can be used in RO and NF plants, such as polyacrylates, organophosphonates, or sodium hexametaphosphate [27]. However, the dosage of antiscalants used to prevent membrane scaling depends on many factors such as type of antiscalant used, the quality and composition of feed water, and other controlled parameters (pH, temperature, and treatment time) [28]. The choice of proper antiscalant to be used for a particular application requires a widely accepted lab-scale inhibitors screening procedure for maintaining both technically and economically feasible treatment process [29].

1.2. Interactions between NOM and hardness in surface water sources and membrane fouling

NOM fouling is considered to be more severe when NOM combines with divalent cations to form metal-NOM complexes. Metal-NOM complexes can form a dense and highly compacted fouling layer on the NF membrane surface [30]. According to Ahn et al. [31], dissolved NOM is not as important in the fouling process, as the divalent cations that interact with the NOM and enhance the aggregation and deposition of foulants on the membranes. Divalent cations are mainly responsible for enhancing the fouling phenomenon, rather than the direct interaction of NOM carboxylate groups with the sulfonyl groups of polyethersulfone (PES) membranes and amino groups of thin-film composite (TFC) polyamide membranes [31].

Many researchers have extensively studied the binding of divalent and monovalent ions to the acidic groups of NOM (Table 1) [3,31,32]. These studies reveal that Ca^{2+} interacts more strongly with NOM to form a thick fouling layer on the membrane surface, in comparison to Mg^{2+} or other ions such as sodium (Na^+). This fouling behavioral difference between calcium and magnesium is associated with the strong inner-sphere complexation capacity for Ca^{2+} and no complexation at all for Mg^{2+}, because of which Ca^{2+} forms stronger complexes with NOM carboxylate groups [31].

Unlike other ions, calcium ions bind specifically with the acidic functional groups of NOM and reduce the negative charge of NOM by forming Ca-NOM complexes [18]. Calcium ions also neutralize the negatively charged membrane surface, which further accelerate the deposition of Ca-NOM complexes onto the partially neutralized membrane surface [31]. The formation of Ca-NOM complexes can result in reduced interchain electrostatic repulsion of NOM, forming small, coiled NOM macromolecules. Also, calcium can act as a medium to form a bridge between these NOM macromolecules, further resulting in a more compact and dense fouling layer on the membrane surface [3].

The concentration of calcium and NOM in feed water and NF membrane surface characteristics are highly responsible in affecting the nature and extent of interactions between them.

Table 1
Research findings of past studies on membrane fouling under different calcium and NOM concentrations in feed water

Paper	Type of feed water (synthetic vs. natural)	Calcium (mg/L as $CaCO_3$)	NOM (mg/L as DOC)	Research findings
[31]	Natural	0.45	2.43	Ca^{2+} associates with the carboxyl groups more strongly than Mg^{2+} due to the looser second hydration shell structure of Ca^{2+}.
[33]	Natural	20.25	3.5–4	High DOC and Ca accumulation was found on the membrane surface in the form of gel on the membrane.
[32]	Synthetic	50	8.24	Severe alginate fouling in the presence of calcium results from calcium induced alginate gel formation at the membrane surface.
[23]	Synthetic	50	10	NOM fouling exhibited greater flux decline with calcium ions, while solution flux curves dominated cake formation model.
[34]	Synthetic	50,100, 200	4.12	With increased calcium addition, cake development becomes the dominant mechanism throughout the filtration step and fouling reversibility is increased with the increase of calcium concentration.
[10]	Synthetic	100	20	Increased flux decline in NF90 membrane in the presence of calcium ions is attributed to the metal-humic complexation and membrane surface roughness.
[35]	Natural	105.5–115.8	6.7–8.7	Increased calcium concentration could cause precipitations in the fouling (cake layer).
[36]	Synthetic	123.5	9.9	Sieving mechanism of the NF90 membrane changed slightly with fouling as the effective pore size became smaller with a larger deviation in pore size after fouling.
[37]	Natural	166.5	2.68	A significant amount of Ca was detected in the membrane acid cleaning disposals; the inorganic-bound Ca was the major foulants. Dissolved organics seemed to accumulate very near the membrane surface and the flat-board-like inorganic matter accumulated next to the organic fouling layer.
[38]	Synthetic	15.62, 31.25, 46.85, 62.5, 125, 250, 556.25	4.12–8.24	Flux decline and irreversible fouling developed during filtration increased with the calcium addition due to the bonding and charge neutralization capacity of calcium on membrane filtration.
[39]	Surface	181.75–1016.75	1.5–6.5	Higher NOM removal efficiencies were obtained with NF90 membrane for all the tested water. Flux decreases in the presence of NOM and decreases further in the presence of both NOM and calcium ions.
[18]	Synthetic	25–250	10	Product water flux due to NOM fouling decreases dramatically as calcium concentration increases.

These interactions can affect the membrane performance in terms of flux decline, hydraulic resistance due to fouling, fouling mechanism, reversibility (or irreversibility), and surface roughness of fouling layer. Several research works have been carried out for investigating the fouling in NF membranes under different feed water quality, specifically concentration of DOC and calcium (Table 1). The reported NF feed water DOC ranged between 1.5 and 20 mg/L and calcium concentration between 0.45 and 1,016 mg/L. However, none of these studies actually investigated fouling mechanism in the feed water containing both extremely high DOC and Ca concentration higher than 100 mg/L.

1.3. Effects of membrane properties on flux decline and membrane fouling

1.3.1. Compaction of NF membranes

Deformation of membrane structure, due to compaction, in the early stages of filtration is a very common phenomenon

in high pressure driven membranes, such as NF and RO. While the membrane is compacting, a significant decline in flux can be observed and also an increased rejection, until the membrane matrix reaches an equilibrium state, that is, permeate flux is constant [40,41]. However, compaction can be both reversible and irreversible in nature. A permanent deformation in the membrane structure results in irreversible compaction, however, when the membrane partially regains its structure, after some relaxation effect, is known as reversible compaction [42].

Hussain et al. [40] studied the compaction effect in NF90 membrane samples by observing the decline in flux with time. The initial flux in the study represented the original membrane permeability as per manufactured characteristics, while the final flux indicated the extent to which the NF membrane can be compacted. It was also found that in case of TFC membranes, the flux is controlled by the active polyamide skin layer and not the polysulfone support layers. The flux was observed to decrease by almost 40% within the experiment time of 2 h, due to compaction [40]. Due to the effect of compaction in TFC membranes, most of the studies for investigation of fouling mechanisms, include a precompaction step before the actual filtration tests. Membranes are precompacted at a higher pressure than the operating pressure to ensure the flux stability during fouling studies [24], and to separate the effects on flux decline due to membrane compaction and fouling.

1.3.2. Membrane surface morphology

Many surface analysis techniques are available for assessing the membrane fouling and cleaning efficiency based on visualization of membrane surface images. Atomic force microscopy (AFM) is the most commonly used technique to characterize the membrane surface morphology and study the surface adhesion – membrane fouling behavior [14,43]. AFM images are also very helpful in evaluating the performance of chemical cleaning procedures. Karime et al. [44] compared the surface of a fouled membrane and the surface of a chemically cleaned membrane, and a remarkable difference in surface roughness (141.19 and 92.32 nm, respectively) was found between both the membranes. AFM image analysis provides several key parameters that can be used to characterize the membrane surface roughness, such as mean plane roughness (R_a – arithmetic average of all surface height deviations measured from the mean plane), root mean squared roughness (R_q – RMS deviation of the peaks and valleys from the mean plane), and surface area difference (change in surface area due to fouling) in nanoscale. Both the mean plane and RMS roughness of membrane surface are quite close to each other, unless there is a large peak observed in the surface analysis which raises the RMS roughness [45].

The surface roughness of membranes obtained from the AFM images have been directly correlated to the intensity of membrane fouling and resulting flux decline. Several researchers have identified increase in flux decline with increase in membrane surface roughness [33,46,47]. Hirose et al. [48] suggested that a linear relationship exists between the mean plane roughness of membrane surface and the permeate flux for cross-linked aromatic polyamide RO membranes. The higher the mean plane roughness, the larger is the surface area for adsorption which increases the deposition of particles onto the membrane surface, further resulting in severe flux decline [46–49]. Particles preferentially get deposited into the valleys of a rough membrane surface causing valley-clogging and resulting in decreased flux [3,16]. Vrijenhoek et al. [46] used the physical parameters obtained from AFM analysis to correlate them with the flux decline data of RO and NF membranes to predict the trend of fouling in membranes. This study identified a flux decline of almost 38%–50% in RO membranes (33.4–52.0 nm) and 14%–47% in NF membranes (10.1–43.3 nm) (increasing flux decline with increasing mean plane surface roughness). The dependency of fouling and flux decline on membrane surface roughness has been elaborated quite evidently in literature. Despite of these efforts, the relationship between the measured surface roughness and resistances offered due to various fouling mechanisms in NF membranes has not been investigated.

1.4. Flux decline and membrane fouling mechanisms

Several mathematical models have been widely used to explain the permeate flux decline due to various fouling mechanisms. Some commonly used models based on various fouling mechanisms in a cross-flow filtration system are complete pore blocking, standard pore blocking, intermediate filtration, and cake filtration [50–52]. The linearized form of Eqs. (1–4 in Table 2) for permeate flow at a constant pressure for each fouling model can be used for data analysis and model identification. The regression coefficient (R^2) can be used as an index to investigate the agreement of experimental data with the used model. The closer the R^2 value of a particular model to 1, the more dominant is the fouling mechanism associated to that model [53,54].

Various factors can affect the flux decline in NF membranes, such as membrane compaction, concentration polarization, adsorption, and pore blockage. Other than built-up of fouling layer on the membrane surface, these phenomena usually occur at much shorter time span from the beginning of filtration. The effect of these factors on the membrane performance can be investigated only after a period of operation. The fouling models (Table 2) do not allow the individual investigation of all these factors. Resistance-in-series model incorporates the effect of each factor affecting the fouling mechanisms in membranes and allows for determinations of various hydraulic resistances.

Table 2
Fouling models

Fouling mechanism	Constant pressure filtration	
Complete pore blocking	$\ln J = \ln J_o - k_b t$	(1)
Gradual pore blocking (standard pore blocking)	$\frac{1}{\sqrt{J}} = \frac{1}{\sqrt{J_o}} + k_s t$	(2)
Intermediate filtration	$\frac{1}{J} = \frac{1}{J_o} + k_i t$	(3)
Cake filtration	$\frac{1}{J^2} = \frac{1}{J_o^2} + k_c t$	(4)

In Eqs. (1)–(4), J is the flux (L/m²/h) at time t (hours), J_o is the initial flux (L/m²/h), and the various k values represent the fouling coefficients.

1.4.1. Resistance-in-series model

Flux decline in a cross-flow pressure driven membrane can be caused by several fouling mechanisms that introduce additional resistance to the flow. The permeate flux decline in NF membranes is most commonly described by resistance-in-series model based on Darcy's law, as given in Eq. (5) as follows [13,14]:

$$J = \frac{\Delta P}{R_t \eta} \tag{5}$$

$$R_t = R_m + R_p + R_g + R_{f,\text{org}} + R_{f,\text{inorg}} + R_{f,\text{irrev}} \tag{6}$$

where ΔP is the pressure difference between the feed and permeate side of the membrane (Pa), R_t is the total resistance (m^{-1}), and η is the dynamic viscosity of the feed solution (Pa. s). In this study, the total resistance (R_t) is equal to the sum of membrane resistance (R_m), concentration polarization layer resistance (R_p), gel layer resistance (R_g), reversible organic pore fouling resistance ($R_{f,\text{org}}$), reversible inorganic pore fouling resistance ($R_{f,\text{inorg}}$), and irreversible pore fouling resistance ($R_{f,\text{irrev}}$) as shown in Eq. (6). Other than the membrane resistance which is always present, all the other resistances are caused due to the various fouling mechanisms mentioned earlier.

The selectivity of the membrane was estimated by the percentage of retention (R) on NF membrane and is given by Eq. (7) as follows:

$$R = \left(1 - \frac{C}{C_o}\right) \times 100\% \tag{7}$$

where R is the retention (%), C is the permeate concentration (mg/L), and C_o is the concentration in the feed solution (mg/L).

1.5. Objectives of study

The objective of this study was to investigate the influence of calcium concentration (principal constituent of water hardness) on the fouling mechanisms in NF90 membrane used to filter high DOC (17 mg/L) water. As to the author's knowledge, the fouling mechanisms of feed water containing such high DOC accompanied with high hardness has not been studied earlier. The study was intended to provide an understanding of the effect of calcium concentration on the reversibility (or irreversibility) of fouling layer in NF90 membrane. The study focused on investigating the change in behavior of fouling mechanisms and resultant surface morphology of fouling layer due to the interactions between calcium, DOC, and NF membrane. The study was carried out to identify the potential dominant mechanism responsible for maximum flux decline and hydraulic resistance to feed flow.

2. Materials and methods

2.1. Synthetic water and chemical reagents

The synthetic water composition used in this study was based on typical surface water quality reported for three rivers (potable water sources) in Manitoba and Ontario, (Canada). The raw water quality of Red River, Rainy River, and Assiniboine River was obtained for past few years (2012–2015). These rivers were observed to be high in DOC and contained wide range of total hardness concentrations, as presented in Table 3. Since DOC and calcium hardness have been reported to cause the most significant fouling in NF membranes [17,23], these two parameters were mainly considered for the preparation of synthetic water. This study was focused on understanding the flux decline and fouling mechanisms due to the interactions of only calcium ions with DOC in the feed water and NF membrane. For that reason, alkalinity, though being an important water quality parameter in surface waters, was not added to the synthetic water.

Sodium alginate was used as a model component for DOC [32,55,56] and calcium chloride for hardness [10] in the synthetic water. Sodium alginate is an anionic polysaccharide (hydrophilic neutral compound) produced by bacteria and algae. Based on the range of DOC reported in the three rivers during (as shown in Table 3), the concentration of sodium alginate used in the synthetic water was 17 mg/L as DOC. The total hardness concentration for the three rivers discussed in this study was reported to be in the range of approximately 40–400 mg/L as $CaCO_3$ and therefore, three different calcium concentrations (50, 200, and 350 mg/L as $CaCO_3$) were selected for the preparation of synthetic water. Both calcium and magnesium are responsible for contributing total hardness in surface water. However, in this study only calcium was considered to be responsible for the total hardness in synthetic water, due to its high complexation capacity with NOM compared with magnesium. Sodium hydroxide (pH 12) and citric acid (pH 4) solutions were used for cleaning the fouled NF membranes. All the chemicals and reagents used for membrane filtration experiments were purchased from Sigma Aldrich, USA, in powder form and stock solutions were prepared using deionized (DI) water.

Table 3
Raw water quality in three rivers in the Canadian Prairie

Source of raw water	DOC (mg/L)		Average DOC	Total hardness (mg/L as $CaCO_3$)		Average hardness
	March	August		March	August	
Red River	10.8	12.35	11.6	376.5	323	350
Assiniboine River	13.8	16.1	15	309	285	200
Rainy River	23.2	8.7	15.95	65	41.6	50

2.2. Laboratory membrane filtration setup

A flat sheet polyamide TFC NF membrane was used for all the experiments in this study (NF90, DOW Filmtec, USA). According to the manufacturer, the membrane rejects 85%–95% of NaCl under the following test conditions: maximum applied pressure of 41 bar and temperature of 45°C. The NF90 membrane has an MWCO (molecular weight cutoff) of 200 Da [57]. NF90 is a commercial tight membrane consisting of a fully aromatic polyamide active layer supported by a porous polysulfone layer reinforced with a nonwoven polyester layer [58,59]. NF90 membranes are negatively charged under any chemical conditions and also the surface roughness of the membrane is considered to be very high (68–70 nm) compared with the surface roughness reported for several other available NF membranes (10.1–43.3 nm) [10].

A cross-flow Sterlitech CF042D membrane filtration cell was used for all the filtration experiments. The internal dimension of the membrane cell was 42 cm^2 as membrane active area and a feed spacer thickness of 7 mm. Besides, the cross-flow filtration setup consists of temperature control system, pumps, feed tank (40-L capacity), pressure gauge and valves, flow meter, digital weighing scale, and automatic data acquisition system (Fig. 1). The temperature control system was used to maintain a constant temperature of feed water at around 21 ± 1°C. The permeate was continuously collected and weighed using a weighing scale to monitor the permeate flux. The system was operated in a closed loop mode, as both the permeate and concentrate were circulated back to the feed tank to maintain a constant feed concentration. The system was designed to operate at a constant pressure and variable flux, however, vice versa can also be done [51]. WTP operate at a constant predetermined flux production and variable pressure conditions.

2.3. Experimental procedure

2.3.1. Membrane precompaction

As a preconditioning step, all membrane samples were soaked for 24 h in DI water [40], prior to running any filtration tests. This preconditioning step removes any preservatives or residuals on the membranes and ensures that the membranes perform as expected. All the membrane samples were precompacted at a constant pressure of 40 bar for 8 h (based on preliminary laboratory studies) to stabilize the flux before running any fouling tests. After the precompaction and relaxation of membranes for 12 h, the flux was measured at an operating pressure of 10 bar for determination of membrane resistance after compaction. The relaxation time was provided to observe any flux restoration due to reversible compaction.

2.3.2. Fouling experiments

The fouling experiments were carried out using three different composition of synthetic waters, where the concentration of sodium alginate was constant (17 mg/L as DOC) and only the concentration of calcium chloride was varied (50, 200, and 350 mg/L as $CaCO_3$). The experiments for each synthetic water composition were carried out in triplicates. Each fouling test was continuously carried out for 3 d, at a constant operating pressure of 10 bar. Also, flux measurements in all the experiments were done at the same operating pressure (10 bar).

The total fouling resistance was determined from the flux obtained in the end of the fouling experiment. After completing the fouling experiment, DI water was used for forward flushing of the membrane cell, without any applied pressure for around 10 min. The flux was measured to determine the resistance due to the presence of concentration polarization layer in the vicinity of membrane surface. The physical cleaning of membrane surface was done by carefully removing the membrane from the filtration cell and gently wiping out the side exposed to the cross-flow, using Kimwipes (Kimberley Clark, USA) [60]. The physical cleaning process removes any gel layer formed due to deposition of foulants on the membrane surface, and hence leaving only foulants deposited into the pores. The flux measured at an applied pressure of 10 bar after physical cleaning was used to determine the gel layer resistance. For chemical cleaning, sodium hydroxide (pH 12) and citric acid (pH 4) solutions were used for the removal of organic and inorganic foulants, respectively, in the membrane pores. A high pH cleaning cycle should be done before the low pH cleaning cycle so as to avoid having the organic material lose their anionic charge. A loss of charge properties may cause the foulant to compact into the membrane and become more difficult to remove [61]. The chemical cleaning process for each solution was carried out for 1 h at a constant applied pressure of 4 bars, so that no permeate is produced with either highly acidic or basic qualities. The flux measured at an applied pressure of 10 bars after each chemical cleaning procedure was used to determine the reversible organic and inorganic pore fouling resistance. After these cleaning steps,

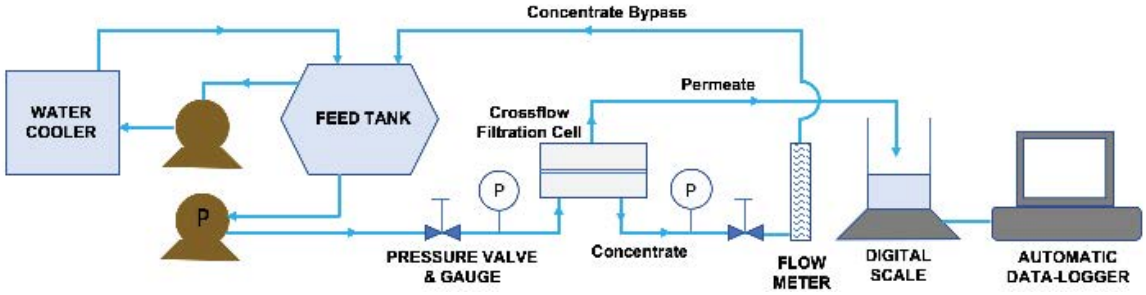

Fig. 1. Schematic diagram of the Bench-scale Experimental Setup.

the remaining resistance due to the presence of irreversible foulants in the membrane pores was determined. For each experiment, all the resistances are measured for membranes fouled and cleaned in one cycle only. The resistance-in-series model was used for the determination of resistances due to various fouling mechanisms observed during the fouling experiments (Fig. 2).

2.4. Analytical methods

A TOC (total organic carbon) analyzer (Teledyne Tekmar TOC Fusion Analyzer, USA) was used to measure the alginate (DOC) content in both the feed and permeate water. The water hardness was determined by using standard EDTA Titration method (Hach, USA) in both feed and permeate water. For DOC and hardness retention measurements, samples of feed and permeate water were collected in the beginning and end of fouling experiments for each synthetic feed composition. Membrane surface roughness was measured using AFM (Veeco D3100, USA) in tapping mode and the images were further analyzed using NanoScope v6 software. The AFM measurements were done on NF membranes, prior to precompaction, after precompaction, and after fouling to observe the changes in membrane surface morphology. The surface roughness presented in the study is the mean plane surface roughness (R_a – arithmetic average of the deviation from the center plane) of different scanning spots.

3. Results and discussion

3.1. Effects of membrane compaction on flux decline

The first part of the study was carried out to investigate the adequate time required to precompact the membrane to obtain a stable flux after a relaxation time of 12 h, that is, membrane compacted beyond that time does not affect the flux obtained after a relaxation time of 12 h. Based on literature studies, the time required for compaction ranges from 2 to 24 h [36,46,62,63]. In this study, the membrane was tested for compaction for 4, 6, 8, and 10 h (Fig. 3) by filtration of DI water through the NF membranes at a constant pressure of 40 bar. Each compaction time was tested in triplicate samples. The flux in the end of the experiment after 4 and 6 h of precompaction was still decreasing, however, for 8 and 10 h of precompaction, the flux was observed to be approaching a constant value.

The membrane resistances have been presented for presoaked virgin membrane (before applying any pressure), after precompaction and precompacted membrane with relaxation of 12 h (Fig. 4). It was observed that the

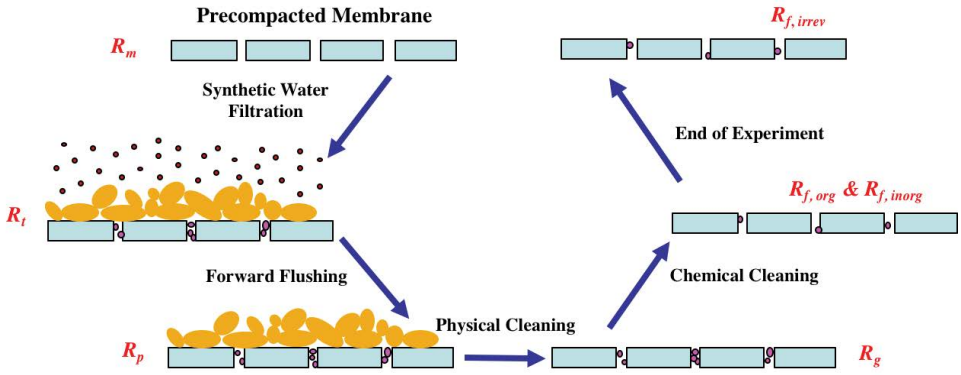

Fig. 2. Flow chart for investigation of resistances due to various fouling mechanisms.

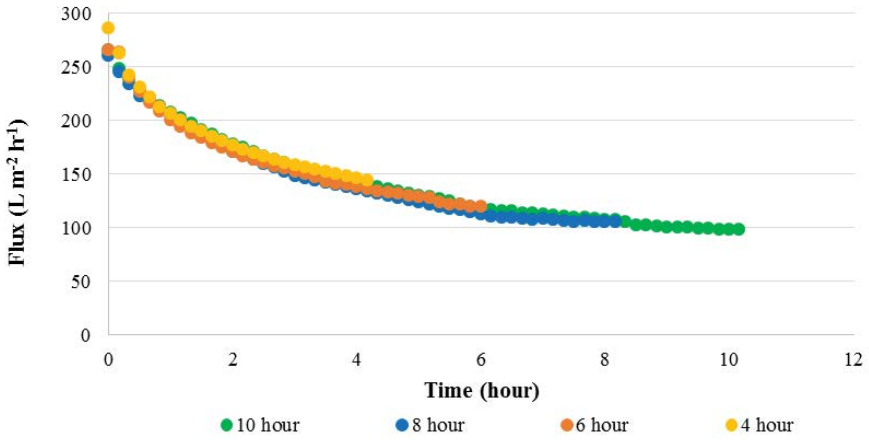

Fig. 3. Flux Decline Curve for different hours of precompaction in NF90 membrane.

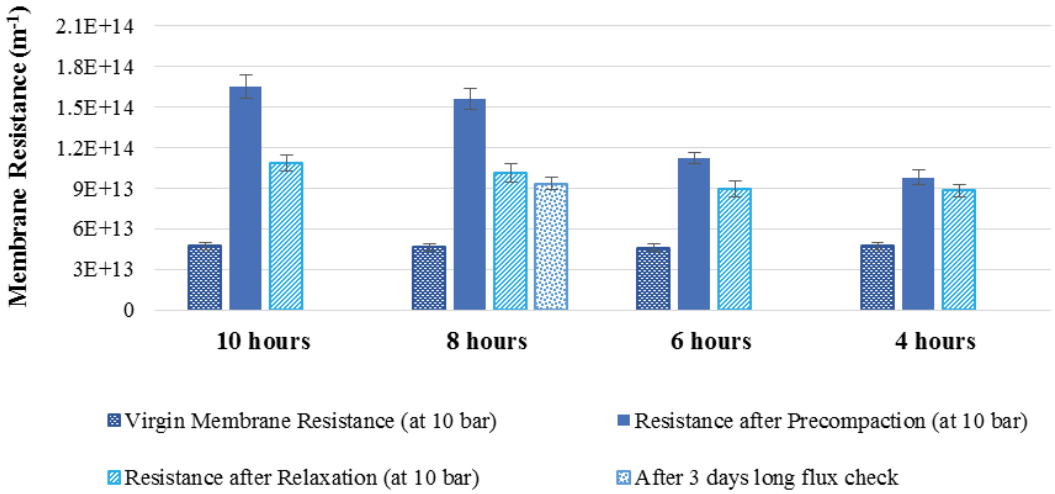

Fig. 4. Change in membrane resistance due to precompaction.

difference in membrane resistance after precompaction as well as relaxation, between 8 and 10 h, was within the standard deviation (5.66E + 12 m^{-1}). Therefore, based on these preliminary laboratory studies, a precompaction time of 8 h was selected for all the membranes, before starting the fouling experiments. Further, the choice (8 h) was also validated by testing the membrane resistance after 3 d DI water filtration. It was observed that there was no significant decline in flux and the membrane resistance was almost constant (Fig. 4).

3.2. *Effect of calcium concentrations on flux decline*

After the precompaction of membranes, the NF membranes were fouled with the synthetic feed waters of varying calcium concentrations.

It was observed that the flux decline in low Ca concentration was more gradual compared with the other two concentrations, throughout the fouling period, and exhibited high total resistance (due to membrane fouling) in the end of the fouling experiment (Fig. 5). For medium and high calcium concentrations, the flux curves were almost parallel to each other, after first few hours of filtration. However, in the end of the fouling experiment, maximum flux decline was observed in the medium Ca concentration and minimum in the high Ca concentration.

The fouling models (Table 2) were used to identify the change in dominance between various fouling mechanisms during the course of filtration experiments. The fouling and regression coefficients were calculated for each calcium concentration for the beginning (1 h) and end (72 h) of the filtration experiments (Tables 4 and 5).

At low Ca concentration, it was observed that in the first hour of filtration, intermediate pore blockage was the most dominant fouling mechanism (R^2 = 0.9993, Table 4). The mechanism changed to cake filtration immediately in the second hour and remained the same throughout the remaining filtration time (R^2 = 0.9787, Table 5). For medium Ca concentration, initially complete pore blockage was dominant (R^2 = 0.9904, Table 4), but changed to intermediate in the second hour and subsequently, cake filtration at the later stages (R^2 = 0.9696, Table 5). However, for high Ca concentration, cake filtration was observed to be dominant since the beginning (R^2 = 0.9986, Table 4), to the end (R^2 = 0.9467, Table 5) of the fouling experiments. These changes in fouling at different stages of filtration were

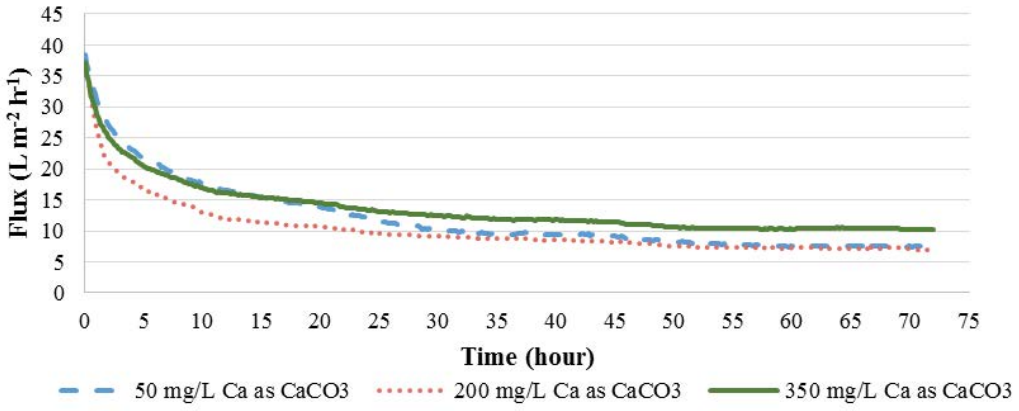

Fig. 5. Flux decline curve for synthetic waters with different calcium concentrations.

Table 4
Model parameters from fouling models for 1 h filtration

Calcium concentration (mg/L as $CaCO_3$)	Complete pore blocking		Gradual pore blocking		Intermediate filtration		Cake filtration	
	k_b	R^2	k_s	R^2	k_i	R^2	k_c	R^2
50	3.63E-03	0.9986	3.07E-04	0.9991	1.04E-04	0.9993	5.94E-06	0.9987
200	5.57E-03	0.9904	4.99E-04	0.9869	1.80E-04	0.9826	1.17E-05	0.9714
350	4.33E-03	0.9956	3.79E-04	0.9973	1.33E-04	0.9983	8.20E-06	0.9986

Table 5
Model parameters from fouling models for 72 h filtration

Calcium concentration (mg/L as $CaCO_3$)	Complete pore blocking		Gradual pore blocking		Intermediate filtration		Cake filtration	
	k_b	R^2	k_s	R^2	k_i	R^2	k_c	R^2
50	2.81E-04	0.8664	4.00E-05	0.9176	2E-05	0.9515	4.00E-06	0.9787
200	2.18E-04	0.7835	3.34E-05	0.8585	2.09E-05	0.9125	4.30E-06	0.9696
350	1.80E-04	0.7952	2.38E-05	0.8501	1.28E-05	0.8927	1.90E-06	0.9467

associated to the changes in calcium concentration and its interaction with alginate molecules and membrane. It was identified that the R^2 values after 1 h filtration for different fouling models were not very different, however, in the end of the fouling experiment, the R^2 values clearly indicate the difference in dominance of fouling mechanism at each calcium concentration.

For all the calcium concentrations, cake filtration was identified to be the most dominant fouling mechanism in the end of the fouling experiments. This finding was in agreement with the findings of Jarusutthirak et al. [23] when calcium chloride ($CaCl_2$) was used as the inorganic model foulant (10 and 50 mg/L as $CaCO_3$) in the synthetic feed water representing the surface water in Thailand. This study identified an increase in flux decline with increase in calcium concentration in the feed water and also cake formation was found to be the most well-fitted model among other models after a filtration period of 8 h. Jarusutthirak et al. [23] reported that when $CaCl_2$ was replaced by $CaCO_3$ in the feed water, the fouling phenomena behaved differently. The inorganic scalant ($CaCO_3$) was found to foul both pores and surface of membrane, but pore blocking was mainly responsible for controlling the flux decline [23].

3.3. Effect of calcium concentrations on resistance

For further understanding of the fouling behavior in the end of the fouling experiment, the resistances due to various fouling mechanisms in each set of fouling experiment were calculated using resistance-in-series model (Fig. 6).

Comparing the total resistance in the end of the fouling experiment for the three different feed waters, medium Ca concentration was observed to exhibit the highest fouling resistance. The resistance due to gel layer formation, concentration polarization, and reversible inorganic pore fouling were observed to behave similar to the total resistance for each feed water. However, the irreversibility of fouling inside the pores behaved completely different and was observed to

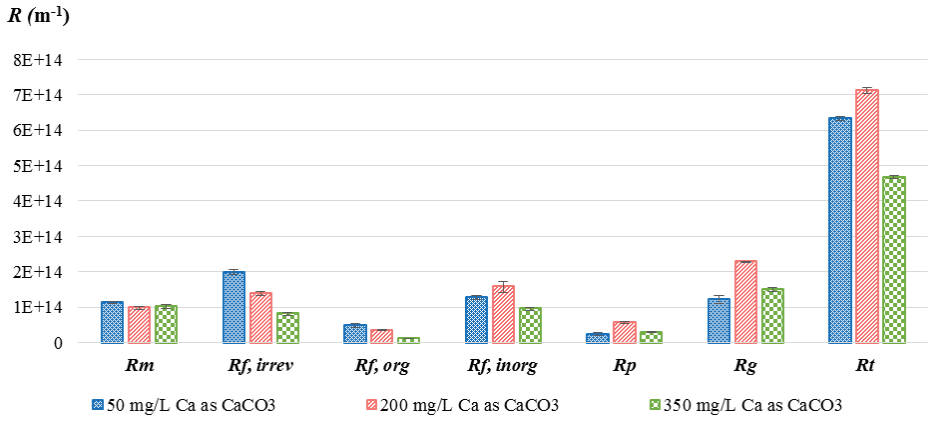

Fig. 6. Resistances due to various fouling mechanisms in NF90 membranes.

be the highest in low Ca and decreased with increasing Ca concentration (Fig. 6).

The change in behavior of fouling mechanisms in NF90 membrane can be explained by the interactions between alginate, calcium, and membrane (Fig. 7). At low Ca concentration, few Ca-alginate aggregates were formed and smaller alginate molecules that could not bind with calcium got deposited in the valleys of the rough NF membrane surface or entered into the pores. This resulted in a minimal gel layer formation with surface roughness of 15.38 nm, and high irreversible and reversible pore fouling resistance (Fig. 9(c)). For medium Ca concentration, although there was complexation and formation of aggregates, the Ca concentration was not high enough to fulfill all the binding sites available on the alginate molecules. This resulted in the formation of a gel layer with relatively high surface roughness of 67.97 nm representative of a complex mixture of Ca-alginate complexes and smaller alginate molecules, offering substantial resistance to feed flow (Fig. 9(d)). However, at high Ca concentration, there was high Ca-alginate complex formation, and the presence of high concentration of calcium ions allowed for intermolecular bridging between the aggregates, forming a cross-linked structure of the fouling layer. This resulted in the formation of a dense and compact gel layer with a surface roughness of 38.17 nm, offering reversible fouling on the membrane surface (Fig. 9(e)). This also demonstrated that gel layer formation becomes the most dominant fouling mechanism, at high calcium concentrations. The consolidated gel layer also caused reduced deposition and fouling inside the pores (Fig. 7).

The hypothesis of the nature of fouling layer demonstrated by comparison of different fouling resistances at each calcium concentration (Fig. 7), correlates with the change in behavior of fouling models during the course of fouling experiments. At low calcium concentration, the intermediate pore blockage in the first hour of filtration explains the clogging of pores by the deposition of foulants on the rough membrane surface. The fouling layer is further smoothened by additional deposition and gel formation on the surface during the remaining filtration time. For medium calcium concentration, the alginate molecules formed complex with calcium and caused immediate flux decline, due to complete pore blockage. Some of the alginate molecules that could not bind with the available calcium were able to enter the pores, causing intermediate pore blockage. Later, the remaining alginates deposited on the membrane surface and the Ca-alginate complexes, resulting in subsequent gel formation with complex foulant structure. At high calcium concentration, the dominance of cake formation model since the beginning of filtration explains the maximum aggregation between calcium and alginate, resulting in a compact fouling layer on the membrane surface.

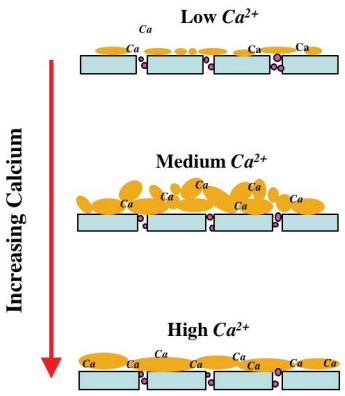

Fig. 7. Behavior of gel layer formation with increasing Ca^{2+} concentration.

3.4. Analyses of membrane surface morphology

The hypothesis on the fouling mechanisms obtained from the resistance-in-series model (resistance calculations) and flux decline models were also validated by the gel layer surface roughness observed using AFM (Figs. 8 and 9). The AFM images observed for clean nonprecompacted membrane identified the very rough surface of NF90 membrane with a surface roughness of 68.9 nm, which was further reduced to a value of 32.2 nm after precompaction. A significant difference was observed in the surface roughness of membranes fouled with feed water containing low, medium and high Ca concentration. The change in surface roughness could be related to the interactions between foulants (alginate and Ca) and membrane surface. The AFM observations suggest that, at low Ca concentration the interaction between foulants and membrane is more adhesive, that is, individual foulants strongly bind with the membrane surface. However, when the Ca concentration is increased, the interaction tends to be more cohesive, that is, Ca-alginate complexation, aggregation, and deposition. Therefore, although the surface roughness in low calcium is lesser compared with that of high calcium, the total hydraulic resistance is vice versa. The higher total hydraulic resistance in low calcium was due to the irreversible nature of fouling, especially in the pores (valley clogging and pore plugging). The value of membrane surface roughness for medium Ca concentration follows the same trend as the measured total resistance (Figs. 6 and 8), that is, the membrane fouled with medium Ca concentration had the highest total resistance and surface roughness. This research was successful in application of AFM to provide a direct relationship between the fouled membrane surface roughness and total hydraulic resistances. The AFM observations of membrane surface roughness support the hypothetical theory presented in this research (as suggested by the experimental results).

Many research studies have concluded that the presence of calcium along with NOM in surface water dramatically decreases the permeate flux, due to the reduced charge of both the NOM and membrane surface [3,7,18,23,32]. Based on literature, the decline in flux and the fouling behavior is attributed to the increase in Ca-NOM complexation, with increasing calcium concentrations. However, in this study, the decline in flux and the resulting hydraulic resistance due to fouling obtained from the experimental results, did not exhibit a linear pattern of increase with increasing calcium concentrations. The maximum flux decline was observed with medium Ca concentration, instead of high Ca concentration (Fig. 5).

The AFM analysis of the fouled membranes indicated that there is a relationship between the total hydraulic resistance and membrane surface roughness (Figs. 6 and 8). Both

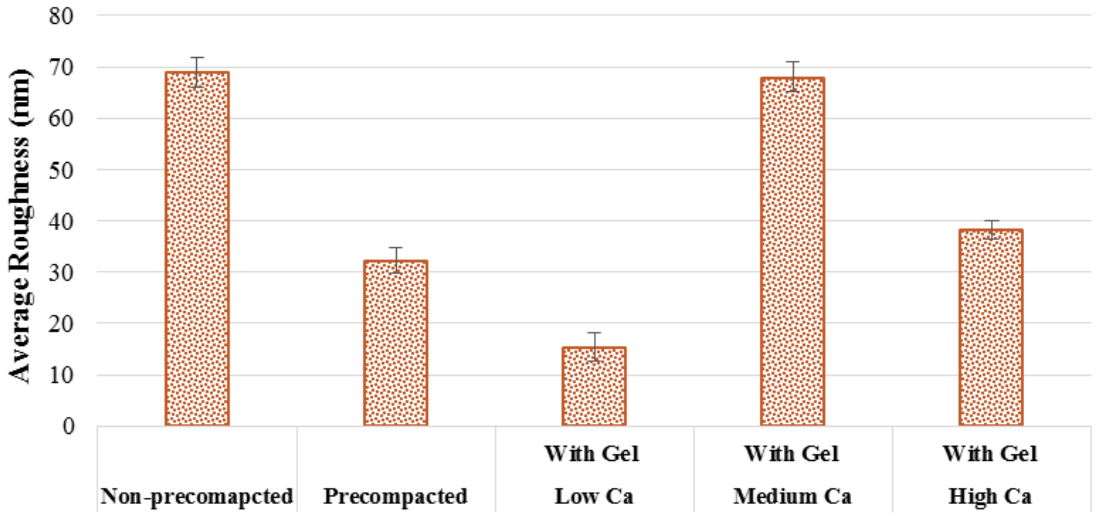

Fig. 8. AFM measured mean plane surface roughness of NF-90 membrane.

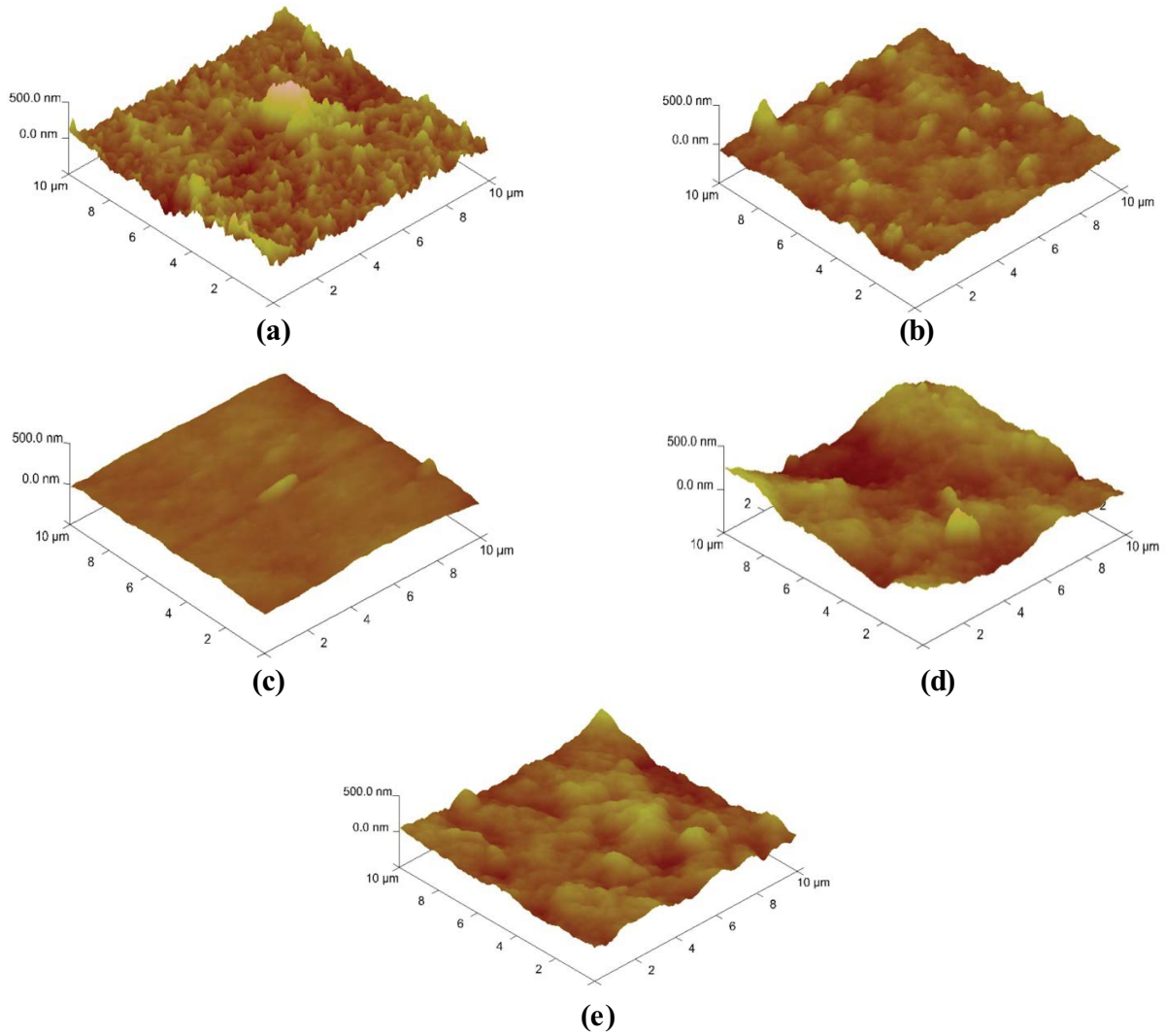

Fig. 9. AFM images of NF-90 membrane surface (a), nonprecompacted (b), precompacted (c), 50 mg/L Ca as $CaCO_3$, (d) 200 mg/L Ca as $CaCO_3$, and (e) 350 mg/L Ca as $CaCO_3$.

experimental results and AFM observations suggested that, at medium Ca concentration the incomplete complexation of calcium with NOM resulted in fouling mechanisms responsible for maximum hydraulic resistance to the feed flow and maximum flux decline.

Calcium is considered to exert more significant effect on the fouling layer when the binding site on NOM is completely saturated, that is, no more complexation after a certain limit of calcium concentration (also known as pseudo-maximum concentration) is reached [7,18]. Also, when there is less calcium available to fulfill the binding sites on NOM, the small-sized NOM and the complexed NOM can form a complex foulant structure, offering high resistance to feed flow. Therefore, it is understood from the experimental results and membrane surface analyses, that to minimize the complexity of the foulant structure and to maximize the reversibility of fouling, the Ca concentration should be just sufficient enough to fulfill all the binding sites available on the NOM in the feed water.

3.5. Results for retention of DOC and hardness

The NF90 membrane was also evaluated for the rejection of organic and inorganic content in the feed water (Fig. 10). Rejection of DOC and hardness by the NF90 membrane was observed to be very high, as specified by the manufacturers. The increase in retention of hardness was observed due to the increasing concentration of calcium in feed water. However, the hardness of permeate water was independent of the calcium concentration in feed water.

3.6. Comparison of NF90 membrane performance using natural and synthetic water

This research was further continued to study the fouling in NF90 membranes used to filter natural surface water – Boyne River which was supplying Stephenfield pilot plant prior to construction of full-scale plant (Manitoba, Canada).

The laboratory bench-scale results for both DOC and hardness removal efficiency using NF90 membrane for filtration of synthetic water (high Ca concentration) were observed to be very similar to that of the natural (Boyne river) water (Table 6). The natural feed water used for the bench-scale study was collected from stage 1 (NF270) effluent of the Stephenfield pilot plant (Table 6); the similar laboratory set-up was used as the one used for this research.

The flux data obtained from the bench-scale experiments using synthetic and natural water, when analyzed for the dominance of fouling mechanism after the first hour of filtration were in agreement with each other (Table 7). It was identified that cake filtration was the most dominant fouling mechanism right from the beginning of both the studies, with regression coefficients of 0.9986 and 0.9923, respectively.

Also, after 1 h of filtration, the total hydraulic resistance measured using synthetic water was found to be coherent with that of natural water, as 1.216 + E14 m^{-1} and 1.250 + E14 m^{-1}, respectively. The flux after 1 h filtration was observed to be 25.24 L/m^2/h (Fig. 5) for synthetic water and 27.19 L/m^2/h for natural water (Fig. 11) [64], at a constant operating pressure of 10 bars and temperature of 21 ± 1°C. The observed flux values, operating pressure and viscosity of feed water (operating temperature) were incorporated in the equation for

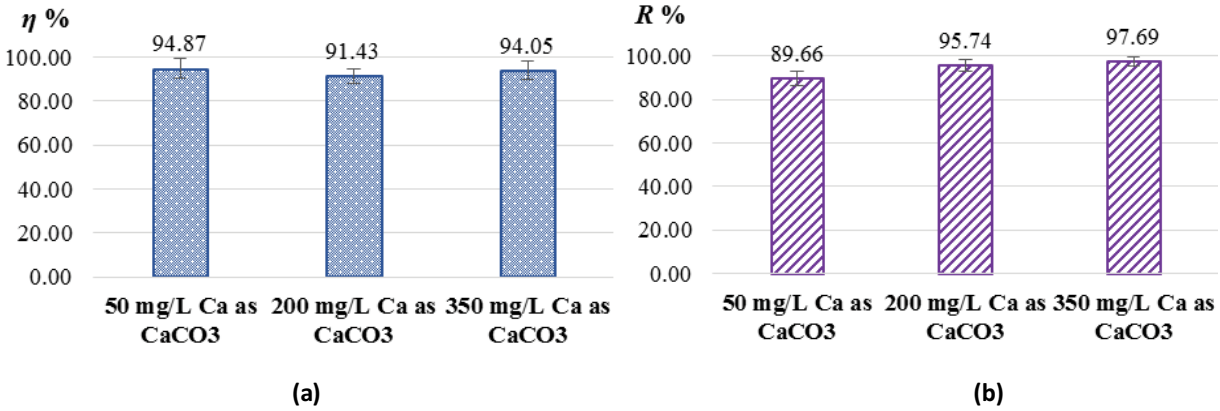

Fig. 10. Retention on NF90 membranes (a) DOC and (b) hardness.

Table 6
Natural and synthetic feed water (high Ca) parameters and removal efficiencies of NF90 membrane

Parameters	Natural water (Boyne river stage 1 effluent)		Bench scale study (synthetic water – high Ca)	
	Feed water	% Removal (early stage)	Feed water	% Removal
DOC (mg/L)	18.6	94.7	17	94.05
Hardness (mg/L as $CaCO_3$)	360	96.0	350	97.7
Alkalinity (mg/L as $CaCO_3$)	305	NA	N/A	N/A
Manganese (mg/L)	1.81	99.7	N/A	N/A

Table 7
Model parameters from fouling models for 1 h filtration of synthetic water (high Ca) and natural (Boyne river) water

Feed water	Complete pore blocking		Gradual pore blocking		Intermediate filtration		Cake filtration	
	k_b	R^2	k_s	R^2	k_i	R^2	k_c	R^2
Synthetic water (high Ca)	4.33E-03	0.9956	3.79E-04	0.9973	1.33E-04	0.9983	8.20E-06	0.9986
Natural water (Boyne River)	1.2121	0.8515	0.0882	0.9165	0.0263	0.9612	0.0012	0.9923

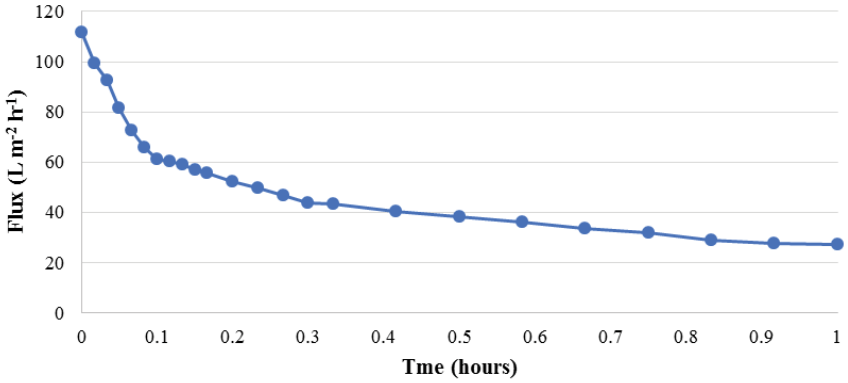

Fig. 11. Flux decline curve for natural water (Boyne river stage 1 effluent) [64].

resistance-in-series model [Eq. (5) in Section 1.4.1] to calculate the total hydraulic resistances for both synthetic and natural water. For filtration of natural water, the membrane was not precompacted before running any fouling test. The similarity in total hydraulic resistance after first hour of filtration and the dominance of cake filtration in both the cases exhibit that Ca-alginate complexation is mainly responsible for the offered resistance. The effect of compaction on flux decline in NF90 membranes will be more evident when used for longer hours of filtration resulting in increased fouling and hydraulic resistance. Some recent observations by Pembina Valley Water Cooperative Inc. from the pilot plant in Stephenfield were used for calculating the total hydraulic resistance after filtration of Boyne river water for 72 h. The Stephenfield pilot plant (or any other WTP) operates at a variable pressure and constant flux, unlike the lab-scale setup that worked on constant pressure and variable flux. The pilot plant operated at a constant flux of 20.41 L/m^2/h, pressure of 2.7 bar, and temperature of 9.4°C for 72 h, to offer a total hydraulic resistance of 3.59E + 13 m^{-1}. This resistance was much lower compared with the total hydraulic resistance observed in this research for synthetic water (high Ca) filtration for 72 h, that is, 4.67E + 14 m^{-1}. This difference was obviously because of the much lower operating pressure (2.7 bar) in the pilot plant compared with the one used in bench-scale study (10 bar) and resistance being directly proportional to the operating pressure [Eq. (5)].

The results of experiments conducted on a bench-scale cross-flow filtration setup using NF90 membranes for synthetic (high Ca) and natural (Boyne river) water, very well correlated with each other. The feed water used in both the studies were from different sources but consisted of similar DOC and hardness concentration. Since the type of feed water used in this research was not natural, but synthetic, the complex nature of natural surface waters can possibly lead to variations in foulants and membrane interaction when operated for a longer period of time. However, the similarity between total hydraulic resistances due to fouling, measured for both synthetic and natural (Boyne river) water, justifies the choice of model parameters in synthetic water. Besides, in both cases (representing high Ca concentration), the cake formation was identified to be the most dominant fouling mechanism. Similar to synthetic water, natural water was also observed to cause less pore fouling compared with membrane surface fouling (Table 7). The consistency in fouling mechanisms and total hydraulic resistance in both Boyne river water (with high alkalinity) and synthetic water with high calcium concentration (without alkalinity) indicates that alkalinity might not play a major role in flux decline and membrane fouling. However, at low or medium calcium concentrations (as used in this research), in the presence of high alkalinity, precipitates smaller than the membrane pore size might be able to enter the pores and cause scale formation, by adsorption and pore plugging. Antiscalant is generally used in WTPs to avoid any scale formation in the system, which might otherwise interfere with the membrane performance and lifetime.

The findings of this study suggest that NF90 membrane, when used in pilot/full-scale systems in Stephenfield WTP are prone to foul easily due to its high surface roughness, and high DOC and hardness in feed water. However, most of the fouling will be on the membrane surface, due to the formation of a compact and dense fouling (gel) layer that will be mostly reversible by regular chemical cleaning procedures.

4. Conclusion

The objective of this study was to investigate the fouling mechanisms in NF membranes for the filtration of

high DOC water with a range of calcium concentration to represent hardness levels typical for Canadian surface water sources. NF90 membranes were fouled with synthetic waters comprising of high alginate concentration (17 mg/L as DOC) and calcium hardness of three concentrations: low 50, medium 200, and high 350 mg/L as $CaCO_3$. To the author's knowledge, there have been no studies conducted on NF membranes for the filtration of water that contains such high concentration of DOC and Calcium. We postulate the following fouling mechanisms for low, medium, and high Ca hardness waters.

- At low Ca concentration, the alginate molecules in the synthetic feed water undergo lesser complexation and aggregation. Most of the alginate molecules and smaller aggregates preferentially accumulate in the valleys of rough membrane surface, due to increased adhesiveness between foulants and membrane. Pore fouling is the dominant fouling mechanism and therefore the fouling exhibit highly irreversible behavior. This fouling mechanism results in low hydraulic resistance and low surface roughness of the membrane.
- At high Ca concentration, the Ca-alginate complexation results in formation of a substantially compact gel layer on the membrane surface, due to high cohesive forces existing between foulants. The fouling layer in this case exhibits reversible fouling behavior with minimal foulants entering the pores (less troublesome). Formation of this gel layer is the dominant fouling mechanism at high calcium concentration, offering low hydraulic resistance and has low surface roughness.
- At medium Ca concentration, the Ca concentration in the feed water was not sufficient enough to fulfill the binding sites on the alginate molecules. Due to which, fewer Ca-alginate complexes were formed and most of the smaller alginate molecules got accumulated along with the complexes on to the membrane surface. The resistance due to gel formation was the dominant fouling mechanism. The gel formed a complex matrix with a very rough surface and therefore offered maximum hydraulic resistance to flow, resulting in maximum flux decline compared with the other two concentrations.
- The fouling mechanisms based on experimental results were consistent with the observed changes in gel layer surface roughness using the AFM images. The surface roughness of the gel layer formed with different calcium concentration was in agreement with the hypothetical theory of calcium ion interaction with DOC and NF membrane surface, proposed in this research.

Literature suggests that the flux decline due to fouling in the presence of DOC increases with increasing calcium concentrations. However, the results of this study identified a dramatic sensitivity to calcium concentration in terms of flux decline and hydraulic resistances. The study demonstrates that the flux decline is not solely dependent on the calcium concentration. Both the concentration of DOC and calcium in feed water affects the complexity of foulant structure formed on the membrane surface, further affecting the reversibility (or irreversibility) of membrane fouling. Also, this study was helpful in identifying that there is no linear relationship between the roughness of the fouling layer and the total resistance offered by the fouled membrane.

Acknowledgments

The authors would like to acknowledge National Sciences and Engineering Research Council (NSERC) and Pembina Valley Water Cooperative Inc. for the financial and technical support provided for the completion of the research work.

Acronyms and Symbols

NOM	—	Natural organic matter
DOC	—	Dissolved organic matter
NF	—	Nanofiltration
RO	—	Reverse osmosis
WTP	—	Water treatment plant
TFC	—	Thin film composite
MWCO	—	Molecular weight cutoff
AFM	—	Atomic force microscopy
DI	—	Deionized water
PES	—	Polyethersulfone
R	—	Retention, %
C	—	Permeate concentration, mg/L
C_o	—	Concentration in the feed solution, mg/L
J	—	Flux, L/m^2/h
J_o	—	Initial flux, L/m^2/h
k	—	Fouling coefficient
R^2	—	Regression coefficient
μ	—	Dynamic viscosity, Pa. s
ΔP	—	Pressure difference between feed and permeate side of membrane, Pa
Da	—	Dalton
R_m	—	Membrane resistance, m^{-1}
R_t	—	Total resistance, m^{-1}
R_P	—	Concentration polarization layer resistance, m^{-1}
R_g	—	Gel layer resistance, m^{-1}
$R_{f,\text{org}}$	—	Reversible organic pore fouling resistance, m^{-1}
$R_{f,\text{inorg}}$	—	Reversible inorganic pore fouling resistance, m^{-1}
$R_{f,\text{irrev}}$	—	Irreversible pore fouling resistance, m^{-1}
R_a	—	Mean plane roughness, nm
R_q	—	Root mean squared roughness, nm

References

[1] A. Mohammad, Y. Teow, W. Ang, Y. Chung, D. Oatley-Radcliffe, N. Hilal, Nanofiltration membranes review: recent advances and future prospects, Desalination, 356 (2015) 226–254.
[2] T. Darton, U. Annunziata, F.V. Pisano, S. Gallego, Membrane autopsy helps to provide solutions to operational problems, Desalination, 167 (2004) 239–245.
[3] A.S. Al-Amoudi, Factors affecting natural organic matter (NOM) and scaling fouling in NF membranes: a review, Desalination, 259 (2010) 1–10.
[4] W. Sun, J. Liu, H. Chu, B. Dong, Pretreatment and membrane hydrophilic modification to reduce membrane fouling, Membranes, 3 (2013) 226–241.
[5] A.R. García, N. Martel, I. Nuez, Short review on predicting fouling in RO desalination, Membranes, 7 (2017) 1–17.
[6] SAMCO, Reverse osmosis and nanofiltration membrane filtration systems: common problems and how to fix them, 04 May 2017. [Online]. Available: https://www.samcotech.com/reverse-osmosis-and-nanofiltration-membrane-filtration-systems-common-problems-and-how-to-fix-them/, Accessed 04 July 2018.

[7] J. Kilduff, S. Mattaraj, G. Belfort, Flux decline during nanofiltration of naturally-occurring dissolved organic matter: effects of osmotic pressure, membrane permeability, and cake formation, J. Membr. Sci., 239 (2004) 39–53.
[8] A. Zularisam, A. Ismail, R. Salim, Behaviours of natural organic matter in membrane filtration for surface water treatment — a review, Desalination, 194 (2006) 211–231.
[9] F. Saravia, A. Klüpfel, A.Z. Richard, F.H. Frimmel, Identification of nanofiltration fouling layer constituents, Desal. Water Treat., 51 (2013) 37–39.
[10] Q. Li, M. Elimelech, Natural organic matter fouling and chemical cleaning of nanofiltration membranes, Water Sci. Technol. Water Supply, 4 (2004) 245–251.
[11] W.R. Bowen, J.S. Welfoot, Modelling the performance of membrane nanofiltration critical assessment and model development, Chem. Eng. Sci., (2002) 1121–1137.
[12] A. Al-Amoudi, R.W. Lovitt, Fouling strategies and the cleaning system of NF membranes and factors affecting cleaning efficiency, J. Membr. Sci., 303 (2007) 4–28.
[13] Y. Kaya, H. Barlas, S. Arayici, Evaluation of fouling mechanisms in the nanofiltration of solutions with high anionic and nonionic surfactant contents using a resistance-in-series model, J. Membr. Sci., 367 (2011) 45–54.
[14] Y. Fang, S.J. Duranceau, Study of the effect of nanoparticles and surface morphology on reverse osmosis and nanofiltration membrane productivity, Membranes, 3 (2013) 196–225.
[15] L.D. Nghiem, P.J. Coleman, C. Espendiller, Mechanisms underlying the effects of membrane fouling on the nanofiltration of trace organic contamina, Desalination, 250 (2010) 682–687.
[16] S. Shirazi, C. Lin, D. Chen, Inorganic fouling of pressure-driven membrane processes - a critical review, Desalination, 250 (2010) 236–248.
[17] R. Liikanen, Nanofiltration as a Refining Phase in Surface Water Treatment, HUT Laboratory of Water and Wastewater Engineering, Helsinki, 2006.
[18] S. Hong, M. Elimelech, Chemical and physical aspects of natural organic matter (NOM) fouling of nanofiltration membranes, J. Membr. Sci., 132 (1997) 159–181.
[19] T. Speth, A. Guses, R. Summers, Evaluation of nanofiltration pretreatments for flux loss control, Desalination, 130 (2000) 31–44.
[20] L. Fan, J. Harris, F. Roddick, N. Booker, Influence of the characteristics of natural organic matter on the fouling of microfiltration membranes, Water Res., 35 (2001) 4455–4463.
[21] J. Lee, S. Lee, M. Jo, P. Park, C. Lee, J. Kwak, Effect of coagulation conditions on membrane filtration characteristics in coagulation–micro-filtration, Environ. Sci. Technol., 34 (2002) 3780–3788.
[22] N. Svenda, B. Gorczyca, Analysis of Nanofilter Fouling in Dual Membrane Plants Supplied by Sufrace Waters with High Dissolved Organic Carbon and Hardness, American Water Works Association Water Quality Technology Conference, New Orleans, 2014.
[23] C. Jarusutthirak, S. Mattaraj, R. Jiraratananon, Influence of inorganic scalants and natural organic matter on nanofiltration membrane fouling, J. Membr. Sci., 287 (2007) 138–145.
[24] A. Schäfer, N. Andritsos, A. Karabelas, E. Hoek, R. Schneider, M. Nystrom, Fouling in Nanofiltration, Nanofiltration – Principles and Applications, Elsevier Science, New South Wales, 2004, pp. 169–239.
[25] C. Ong, P. Goh, W. Lau, N. Misdan, A. Ismai, Nanomaterials for biofouling and scaling mitigation of thin film composite membrane: a review, Desalination, 393 (2016) 2–15.
[26] W. Ang, A. Mohammad, A. Benamor, N. Hilal, C. Leo, Hybrid coagulation–NF membrane process for brackish water treatment: effect of antiscalant on water characteristics and membrane fouling, Desalination, 393 (2016) 144–150.
[27] J. Landaburu-Aguirre, R. García-Pacheco, S. Molina, L. Rodríguez-Sáez, J. Rabadán, E. García-Calvo, Fouling prevention, preparing for re-use and membrane recycling. Towards circular economy in RO desalination, Desalination, 393 (2016) 16–30.
[28] M. Papapetrou, A. Cipollina, U. Commare, G. Micale, G. Zaragoza, G. Kosmadakis, Assessment of methodologies and data used to calculate desalination costs, Desalination, 419 (2017) 8–19.
[29] K. Popov, G. Rudakova, V. Larchenko, M. Tusheva, S. Kamagurov, J. Dikareva, N. Kovaleva, A comparative performance evaluation of some novel (green) and traditional antiscalants in calcium sulfate scaling, Adv. Mater. Sci. Eng., (2016) 1–10.
[30] A. Seidel, M. Elimelech, Coupling between chemical and physical interactions in natural organic matter (NOM) fouling of nanofiltration membranes: implications for fouling control, J. Membr. Sci., 203 (2002) 245–255.
[31] W.Y. Ahn, A.G. Kalinichev, M.M. Clark, Effects of background cations on the fouling of polyethersulfone membranes by natural organic matter: experimental and molecular modeling study, J. Membr. Sci., 309 (2008) 128–140.
[32] S. Lee, W.S. Ang, M. Elimelech, Fouling of reverse osmosis membranes by hydrophilic organic matter: implications for water reuse, Desalination, 187 (2006) 313–321.
[33] W. Song, V. Ravindran, B.E. Koel, M. Pirbazari, Nanofiltration of natural organic matter with H2O2/UV pretreatment: fouling mitigation and membrane surface characterization, J. Membr. Sci., 241 (2004) 143–160.
[34] K. Katsoufidou, S. Yiantsios, A. Karabelas, Experimental study of ultrafiltration membrane fouling by sodium alginate and flux recovery by backwashing, J. Membr. Sci., 300 (2007) 137–146.
[35] A.S. Gorzalski, O. Coronell, Fouling of nanofiltration membranes in full-and bench-scale systems treating groundwater containing silica, J. Membr. Sci., 468 (2014) 349–359.
[36] C. Bellonaa, M. Marts, J. Drewes, The effect of organic membrane fouling on the properties and rejection characteristics of nanofiltration membranes, Sep. Purif. Technol., 74 (2010) 44–54.
[37] E. Gwon, M. Yu, H. Oh, Y. Ylee, Fouling characteristics of NF and RO operated for removal of dissolved matter from groundwater, Water Res., 37 (2003) 2989–2997.
[38] S. Jamal, S. Chang, H. Zhou, Filtration behaviour and fouling mechanisms of polysaccharides, Membranes, 4 (2014) 319–332.
[39] A. Rubia, M. Rodríguez, V. León, D. Prats, Removal of natural organic matter and THM formation potential by ultra- and nanofiltration of surface water, Water Res., 42 (2008) 714–72.
[40] Y. Hussain, M. Al-Saleh, S.S. Ar-Ratrout, The effect of active layer non-uniformity on the flux and compaction of TFC membranes, Desalination, 328 (2013) 17–23.
[41] Y. Hussain, M. Al-Saleh, A viscoelastic-based model for TFC membranes flux reduction during compaction, Desalination, 344 (2014) 362–370.
[42] C. Vishvanathan, B. Marsono, B. Basu, Removal of THMP by nanofiltration: effects of interference parameters, Water Res., 32 (1998) 3527–3538.
[43] Q. Li, M. Elimelech, Organic fouling and chemical cleaning of nanofiltration membranes: measurements and mechanisms, Environ. Sci. Technol., 38 (2004) 4683–4693.
[44] M. Karime, S. Bouguechab, B. Hamrounia, RO membrane autopsy of Zarzis brackish water desalination plant, Desalination, 220 (2008) 258–266.
[45] K. Boussu, B.V.D. Bruggen, A. Volodin, J. Snauwaert, C.V. Haesendonck, C. Vandecasteele, Roughness and hydrophobicity studies of nanofiltration membranes using different modes of AFM, J. Colloid Interface Sci., 286 (2005) 632–638.
[46] E. Vrijenhoek, S. Hong, M. Elimelech, Influence of membrane surface properties on initial rate of colloidal fouling of reverse osmosis and nanofiltration membranes, J. Membr. Sci., 188 (2001) 115–128.
[47] C. Hobbs, J. Taylor, S. Hong, Effect of surface roughness on fouling of RO and NF membranes during filtration of a high organic surficial groundwater, J. Water Supply Res. Technol. AQUA, 55 (2006) 559–570.
[48] M. Hirose, H. Ito, Y. Kamiyama, Effect of skin layer surface structures on the flux behaviour of RO membranes, J. Membr. Sci., 121 (1996) 209–215.

[49] E. Hoek, S. Bhattacharjee, M. Elimelech, Effect of membrane surface roughness on colloid-membrane DLVO interactions, Langmuir, 19 (2003) 4836–4847.
[50] C. Jarusutthirak, S. Mattaraj, R. Jiraratananon, Factors affecting nanofiltration performances in natural organic matter rejection and flux decline, Sep. Purif. Technol., 58 2007 68–75.
[51] A. Abdelrasoul, H. Doan, A. Lohi, A mechanistic model for ultrafiltration membrane fouling by latex, J. Membr. Sci., 433 (2013) 88–99.
[52] E. Iritani, N. Katagiri, Developments of blocking filtration model in membrane filtration, Kona Powder Part. J., 33 (2016) 179–202.
[53] E. Garravanda, C.N. Mulligan, C.B. Laflamme, G. Clairet, Investigation of the fouling effect on a commercial semi-permeable membrane in the pressure retarded osmosis (PRO) process, Sep. Purif. Technol., 193 (2017) 81–90.
[54] Y. Lin, Effects of organic, biological and colloidal fouling on the removal of pharmaceuticals and personal care products by nanofiltration and reverse osmosis membranes, J. Membr. Sci., 542 (2017) 342–351.
[55] M.A. Zazouli, S. Nasseri, M. Ulbricht, Fouling effects of humic and alginic acids in nanofiltration and influence of solution composition, Desalination, 250 (2010) 688–692.
[56] Y. Xin, M.W. Bligh, A.S. Kinsela, Y. Wang, T.D. Waite, Calcium-mediated polysaccharide gel formation and breakage: Impact on membrane foulant hydraulic properties, J. Membr. Sci., 475 (2015) 395–405.
[57] D. Filmtec, Dow Water & Process Solutions, 01 December 2016. [Online]. Available: http://msdssearch.dow.com/PublishedLiteratureDOWCOM/dh_0979/0901b80380979557.pdf?filepath=liquidseps/pdfs/noreg/609-50106.pdf&fromPage=GetDoc.
[58] S. Yüksel, N. Kabay, M. Yüksel, Removal of bisphenol A (BPA) from water by various nanofiltration(NF) and reverse osmosis (RO) membranes, J. Hazard. Mater., 263 (2013) 307–310.
[59] A. Azaïs, J. Mendret, S. Gassara, E. Petit, A. Deratani, S. Brosillon, Nanofiltration for wastewater reuse: counteractive effects of fouling and matrice on the rejection of pharmaceutical active compounds, Sep. Purif. Technol., 133 (2014) 313–327.
[60] K. Listiarini, W. Chun, D.D. Sun, J.O. Leckie, Fouling mechanism and resistance analyses of systems containing sodium alginate, calcium, alum and their combination in dead-end fouling of nanofiltration membranes, J. Membr. Sci., 344 (2009) 244–251.
[61] N. Porcelli, S. Judd, Chemical cleaning of potable water membranes: a review, Sep. Purif. Technol., 71 (2008) 137–143.
[62] S. Lee, J. Cho, M. Elimelech, A novel method for investigating the influence of feed water recovery on colloidal and NOM fouling of RO and NF membranes, Environ. Eng. Sci., 22 (2005) 496–509.
[63] M. Mamun, S. Bhattacharjee, D. Pernitsky, M. Sadrzadeh, Colloidal fouling of nanofiltration membranes: development of a standard operating procedure, Membranes, 7 (2017) 1–19.
[64] I. Moran, B. Gorczyca, Mechanism of Fouling on Four Different NF Membranes, American Membrane Technology Association, San Antonio, 2016.